Available online at www.sciencedirect.com
ScienceDirect
Journal of the European Ceramic Society 30 (2010) 1069–1078
www.elsevier.com/locate/jeurceramsoc

Review

EPD kinetics: A review

Begoña Ferrari *, Rodrigo Moreno

Instituto de Cerámica y Vidrio, CSIC, c/Kelsen, no 5, Cantoblanco, Madrid E28049, Spain

Available online 27 September 2009

Abstract

The colloidal approach has been studied as an essential step in the tailoring of ceramic nanostructures, but most colloidal processes are limited by the complexity of preparation of highly concentrated and stable suspensions of nanoparticles and their fast ageing. Electrophoretic deposition (EPD) stands out as the most appropriate colloidal process to produce ceramic structures using low solid content sols and suspensions (<1 g/l). This characteristic drastically increases its range of technological applicability to nanoparticle assembly, becoming an alternative to the evaporative coating processes. Modelling of this direct electrically driven assembly process is key for its application to the performance of new materials on length scales of approximately 1–100 nm. In this paper, the key contributions in this field to process control and development of the electrophoretic kinetics equation are summarised.

Keywords: Electrophoretic deposition; Shaping; Suspension; Surfaces

Contents

1. EPD as a nanotechnology approach

Research on nanoscience and nanotechnology is motivated by the fact that control of the nanostructure of materials results in enhanced properties at the macroscale. Major efforts have been made to establish nanoparticle synthesis and to develop specific techniques to characterise such materials.[1] Joining both areas of knowledge, assembly strategies (shaping, compaction and sintering processes) have also received special attention, becoming a relevant research objective of this decade.[2]

The production of nanostructured ceramic materials is complex since the conventional processing methods (pressing and hot-pressing) are completely inadequate. The use of dry nanopowders requires special equipment to avoid agglomeration, flowing and float problems as well as a high health risk. Most of these problems are solved if powders are immersed in a liquid medium. The colloidal approach has been studied as an essential step to the tailoring ceramic nanostructures. Special attention has been addressed to binder-free processes (binder < 1 wt.%) and those suitable for near net shape manufacturing of complex-shaped ceramics. Colloidal processes are limited by the hardening performance of highly concentrated and stable suspensions of nanopowders.[3] Concentrated suspensions are needed to improve density and speed up the formation of nanostructure compacts. Among these routes, EPD stands out as a powerful and versatile colloidal process to address the need for inexpensive and mass production of films using suspensions with low concentration (<1 g/l). This drastically increases its range of applicability competing with other non-colloidal techniques, such as evaporative coating processes (thermal evaporation,

* Corresponding author.
E-mail address: bferrari@icv.csic.es (B. Ferrari).

0955-2219/$ – see front matter © 2009 Elsevier Ltd. All rights reserved.
doi:10.1016/j.jeurceramsoc.2009.08.022

electron beam deposition (EBD), ion-assisted deposition (IAD), plasma spraying, etc.).

In most of these coating processes, the transport of small particles by which colloidal forces overcome gravitational forces is mainly governed by Brownian motion, resulting in completely random particle–particle and particle–substrate collision. In electrically driven processes, a directional force (external electric field) is applied, leading to 2D and 3D ordered structures at the nanoscale.[4–7]

R&D activities related to EPD of nanoparticles are in continuous expansion both in industry and academia. Over the past 10 years, a great effort has been made in the field of predictive analytical and numerical modelling of the EPD process, in order to change the empirical trial-and-error approach which dominates the experimental work in this area.[6] New tools such as pair potential modelling, atomic force microscopy (AFM) in liquid media,[8–11] and electrochemical techniques[12–14] are suitable for determining nanoparticle behaviour and the energy barriers developed at the electrode surface during nanoparticle assembly, and hence the process performance should be controlled and predictable.

The aim of this paper is to review the research efforts of the scientific community in this field, describing the parameters which affect electrophoretic deposition morphology and yield. To this end, the evolution and contributions of different authors to the kinetics expression for the process are described.

2. Key suspension parameters

The EPD process is based on the migration and later deposition of charged particles in a stable suspension, induced by the application of an electric field between two electrodes. Particle packing by solvent evaporation is the common compaction mechanism in several shaping processes such as dipping, spin coating and tape casting. Solvent evaporation in EPD is preceded by the electrically assisted formation of a cohesive layer of particles which reproduces the shape of the work electrode. Consequently, deposit yield and particle packing in electrophoresis not only depend on the stability and the solids content of the suspension, but also on the aggregation and the arrangement of the particles on the electrode surface. The performance of EPD in producing homogeneous and reliable films strongly depends on the particle surface chemistry, the behaviour of the surface–liquid interfaces under an electric field, and the development of particle–particle and particle–substrate networks during particle assembly. Fig. 1 schematizes the evolution of particles and related ionic clouds in a stable suspension (a), under the effect of an electric field (b), and during aggregation close to the electrode (c).

Suspension properties, such as conductivity, zeta potential, solid content, viscosity, etc., are key parameters of the EPD process. The colloidal systems used must be stable, meaning that the particles have to maintain dispersed throughout the medium so they can move towards the electrode independently of each other. Then, particles can deposit separately, without agglomerates, keeping open the possibility of their rearrangement during packing through the action of an electric

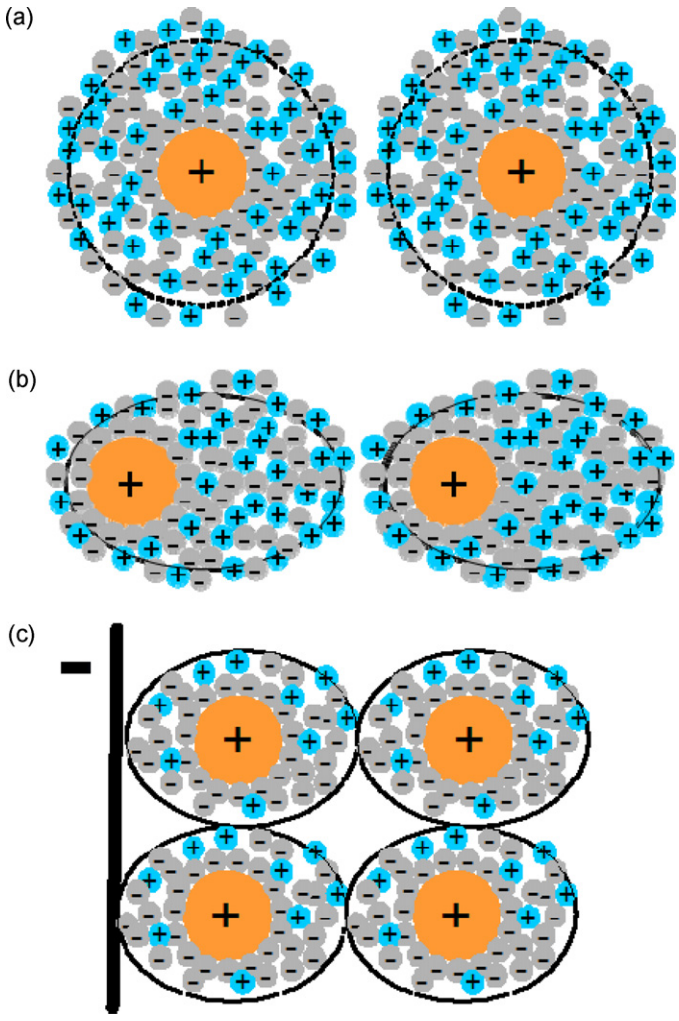

Fig. 1. Scheme of particles dispersed electrostatically (a), distorted double-layers due to the shear action of the fluid during the electrophoretic motion of particles in the bulk suspension (b), and change of the ionic and particles concentration in the electrode boundary (c).

field, similarly to the deposit formation by gravitational forces (sedimentation).[15,16]

Although the necessary requirement for EPD is that suspended particles must have an elevated electrophoretic mobility, conductivity also determines the viability[17] and the development of the process.[11,18] In fact, suspension conductivity is determined by the number of charge carriers (ions and/or particles) and hence, it is directly related to the deposition yield. So, EPD must be performed considering a compromise between high particle mobility and low particle charge per unit weight.[17]

3. Particles arrangement and electric conditions

The principles of electrophoresis have been known since the last century, but particle arrangement in cohesive deposits is not so well-understood.[19–21] The second stage of the EPD process is a matter of controversy and, the debate related to both particle aggregation and their arrangement at the electrode surface is still open to further detailed research in different systems.

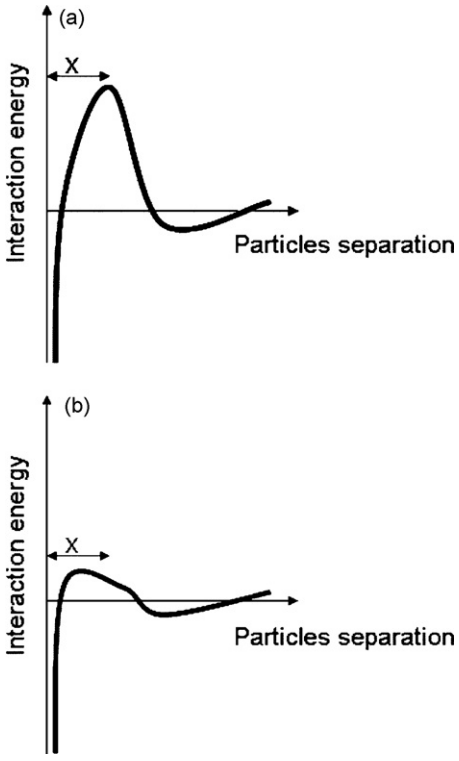

Fig. 2. Potential energy evolution vs. particles distance for surfaces dispersed by an electrostatic mechanism. (a) High energy barrier and (b) low energy barrier.

EPD depends on the charge of the particles in order to promote particle motion, but in addition electrophoretic mobility is related to the Debye length, which determines the minimum force required to promote the coagulation/deposition of particles. Several hypotheses, such as particle neutralization or particle coagulation due to the formation of ions or polymers by means of electrode reactions, have been rejected as the main causes of deposition.[20,22] The most developed theory considers that deposition occurs via double-layer distortion and thinning during electrophoresis, followed by the coagulation of particles under the application of an electric field (Fig. 1).[22] Fig. 2 shows the evolution of the potential energy diagrams vs. the distance between two charged surfaces due to a high (a) or low (b) electrostatic interaction.[23]

In relation to this, the electric field has to be able to develop enough force to overcome the repulsion between particles during deposition (Fig. 2). Proposed causes of changes of the chemical equilibrium of particles at the electrode boundary as a consequence of the application of the electric field, are[24] the increase on solid concentration, the diffusion movement of particles and co-ions,[25–27] co-ion depletion[28] or counterion migration towards the counterelectrode.[11] All these phenomena affect the deposition yield when high conductivity suspensions, high particle sizes, high applied voltages or high solid loadings were considered.[11] In fact, ceramic suspensions are complex systems containing not only particles and ions, but also deflocculants, surfactants, binders, gelling agents, etc. Each component has an important role in the suspension formulation and changes the morphology of the particle arrangement. The determining effect

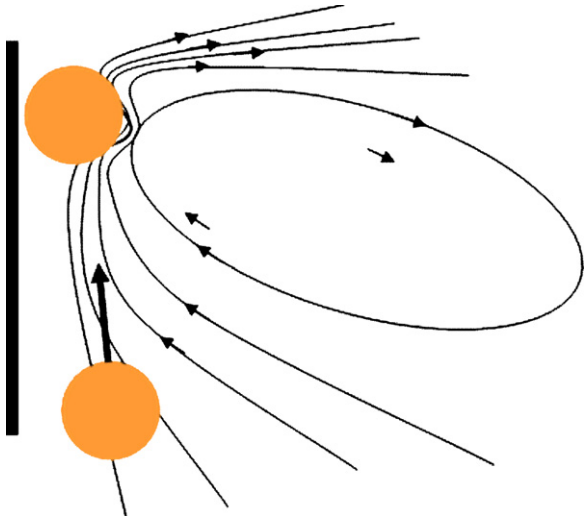

Fig. 3. Hydro-dynamic forces developed over the particles close to the surface electrode.

of the suspension additives in EPD performance and material properties has also been discussed in different studies.[12,29–32]

On the other hand, techniques such as image analysis have been adapted to track and predict the movement of a multitude of particles, verifying that aggregation takes place and the particles form densely packed planar clusters. The aggregation of particles has been modelled by means of different mechanisms, i.e. electrohydrodinamic[33] or electro-osmosis,[34] to explain how the movement of the fluid also pushes particles together near the electrode (Fig. 3). Recently, Ji et al.[16] have measured experimentally a higher densification of deposits under potentiostatic conditions when the electric field and the suspension conductivity are increased, in agreement with the electro-osmotic effect of the liquid over particle aggregation proposed by Solomentsev.[33]

Finally, the electrode surface also plays an important role in the whole EPD process, being the key parameter for the final arrangement of the particles. Polarizable or blocking electrodes exhibit a substantial interface resistance, giving a significant potential drop near the electrodes (i.e. activation overvoltage, concentration overvoltage),[8,20] the voltage gradient in the suspension being smaller than expected. The system becomes unstable such those particles near the electrode alter the local electric field, and fluctuations in the resistance of the interface or the suspension will cause large variations in the distribution of the electric field between the electrodes. However, a nonpolarizable electrode is characterised by an infinitesimally small resistance at the interface. The potential drop between the electrodes therefore occurs entirely in the bulk suspension, resulting in a maximum effective electric field.

Furthermore, when current is passing through the electrode, electrochemical reactions can seriously decrease the efficiency of the process and the uniformity of the deposits. To date, these problems have been addressed technologically by designing an adequate substrate structure, such as graphite or molybdenum porous substrates (e.g. the pore size is fixed in order to promote the oxygen bubbling produced due to water electrolysis), or by studying the passivation range of selected metal substrates.[12,21]

Theoretical electrokinetic models of electrophoresis demonstrate that particle motion occurs near electrodes under a variety of conditions (DC and AC fields with different frequencies).[35,36] In relation to this, recent efforts have been devoted to minimizing the effects of electrode reactions in the deposited materials, specifically in aqueous media, applying DC pulses[37] and AC asymmetric fields.[38] In those cases, frequency is added to time and voltage as electrical parameters to be considered in the kinetics. Studies concerning AC electrophoresis have been performed which indicate a decrease in the deposition yield with an increase in the frequency,[39,40] while demonstrating advantages such as the material deposition occurring at both electrodes. Now, further research work is needed to determine the role of particles–substrate interaction under an electric field, to predict particle arrangement and to design micro and nano-pattern materials.

4. Kinetics approaches: the evolution of the EPD equation

The first model of EPD kinetics was proposed by Hamaker in 1940 (Eq. (1)) for electrophoretic cells with planar geometry.[15] It relates the deposited mass per unit area, m (g), with slurry properties, such as suspension concentration, C_s (g cm^{-3}), and electrophoretic mobility, μ (cm^2 s^{-1} V^{-1}), with physical and electrical conditions imposed on the system such as electric field, E (V cm^{-1}), deposition area, S (cm^2), and deposition time, t (s):

$$m = C_s \mu S E t \tag{1}$$

A similar expression was deduced in 1991 by Hirata et al.[41] based on the application of Faraday's law to the deposition process, considering the particles as the unique charge carriers in the suspension.

The linear variation of deposited mass with deposition time requires that the parameters of Eq. (1) remain unchanged with time. This fact limits the application of the Hamaker expression to short deposition times.

Sarkar and Nicholson[22] analysed the dependence of kinetics on some of the EPD experimental conditions. They firstly introduce an efficiency factor or "sticking parameter", $f \leq 1$ (i.e. if all the particles reaching the electrode take part in the formation of the deposit $f = 1$) to quantify the effect of the undetermined process of deposition. Referring the Hamaker equation (Eq. (1)), they quantified the effect of the variation of particle concentration on the EPD kinetics.

In the early stages of the process the variation of bulk solid concentration in the suspension is negligible, since only a minor fraction of the powder is being deposited. Hence, for infinitesimal intervals of time the Hamaker equation always holds, so that:

$$\frac{dm}{dt} = f \mu S E C_s \tag{2}$$

The amount of powder extracted from the bulk suspension becomes significant for longer times, and consequently C_s decreases. In this case, the deposited mass and the solid content are expressed by

$$m = V(C_{s,0} - C_s) = \frac{m_0}{C_{s,0}}(C_{s,0} - C_s) \tag{3}$$

where $C_{s,0}$ (g cm^{-3}) is the initial solid content of the suspension, V (cm^{-3}) is the volume of suspension considered constant, and m_0 (g) is the initial mass of powder in suspension. All of them are related by the expression:

$$C_{s,0} = \frac{m_0}{V} \tag{4}$$

Eq. (3) gives

$$C_s = C_{s,0}\left(1 - \frac{m}{m_0}\right) \tag{5}$$

Combining Eqs. (2) and (5):

$$\frac{d}{dt}\left(\frac{m}{m_0}\right) = \frac{1}{\tau}\left(1 - \frac{m}{m_0}\right) \tag{6}$$

where τ defines a characteristic time scale given by

$$\tau = \frac{V}{f \mu S E} \tag{7}$$

The inverse value of the characteristic time was defined by Sarkar and Nicholson as a universal parameter, k, named the "kinetics parameter".

If no sedimentation occurs, and the only change of concentration is the mass of powder deposited by EPD, for an initial time, $t = 0$, the deposited mass is $m(0) = 0$, which leads to the solution of Eq. (6):

$$m(t) = m_0(1 - e^{-t/\tau}) \tag{8}$$

This equation for EPD kinetics has been widely applied by Sarkar and Nicholson,[22] and completes the first description proposed by Zhang et al.[42] in 1994, concerning the incorporation of changes in particle concentration in EPD kinetics.

Eq. (8) can be reduced to the Hamaker model for short times, and it is widely accepted in the literature. In recent years several authors have proposed different mathematical models based on this equation to describe the deep electrophoretic penetration and deposition of ceramics in porous substrates,[43–47] to determine deposit thickness,[48] or to control the homogeneity of the porous distribution in a ceramic membrane.[49]

Furthermore, the Sarkar and Nicholson model predicts deviations from linearity occurring when EPD is carried out under constant-voltage conditions, and the deposit resistivity is higher than that of the suspension. In this case, the electric field strength applied to the suspension can be considered to be:

$$E = \frac{\Delta\psi}{L + \delta((\rho_s/\rho_d) - 1)} \tag{9}$$

where $\Delta\psi$ (V) is the potential drop between the electrodes, L (cm) the distance between electrodes, ρ_s and ρ_d (Ω cm) are the resistivities of the suspension and the deposit respectively, the deposit thickness, δ (cm), being defined as follows:

$$\delta = \frac{V_d}{S} = \frac{m/C_d}{S} \tag{10}$$

where V_d (cm^3) is the deposit volume and C_d ($g\,cm^{-3}$) the deposit concentration.

Combining Eqs. (9) and (10), yields:

$$E = \frac{\Delta\psi}{L + R'm} \tag{11}$$

where R' is a constant, the value of which is given by

$$R' = \frac{(\rho_s/\rho_d) - 1}{C_d S} \tag{12}$$

Combining Eqs. (2), (3) and (9), yields:

$$\frac{d}{dt}\left(\frac{m}{m_0}\right) = k'\left(1 - \frac{m}{m_0}\right)\frac{\Delta\psi}{L + R'm} \tag{13}$$

where k' is a redefined "kinetics parameter":

$$k' = \frac{fS\mu}{V} \tag{14}$$

Solving Eq. (13) with similar boundary conditions to Eq. (6), gives

$$R'm(t) + (R'm_0 + L)\ln\left(\frac{m_0 - m(t)}{m_0}\right) + k'\Delta\psi t = 0 \tag{15}$$

Eq. (15) is a general expression to describe the deposition kinetics. It reduces to Eq. (8) when the resistivity of the deposit is similar to that of the suspension ($\rho_s = \rho_d$).

Otherwise, the authors point out, based on Eq. (15), that the shaping of thick deposits involves the preparation of more concentrated suspensions than allowed for the Hamaker model, but they did not quantify this effect. More recently, Biesheuvel et al.[19] have described a deposit growth model, based on the Kynch theory of sedimentation for planar and cylindrical geometries. This theory describes the bulk effect of particle motion in transport phenomena near the deposition electrode, based on the expression of the mass balance of the suspension-deposit boundary evolution, resulting in:

$$\frac{d\delta}{dt} = -v\frac{\phi_s}{\phi_{d-}\phi_s} \tag{16}$$

where v ($cm\,s^{-1}$) is the electrophoretic rate of particles close to the electrode, ϕ_d is the volumetric fraction of the deposit, and ϕ_s is the volumetric fraction of the suspension.

This growth theory is limited to explaining the evolution of the deposit-suspension boundary, and correspondingly the system studied was identified as a non-stirred and electrically neutral suspension. As a consequence, some phenomena occurring during the EPD process were neglected, including the decrease of particle concentration, the movement of particles by diffusion, and the local changes of the charge on the electrodes, both on the particle surface and its surrounding ionic clouds. Hence, as in the Sarkar and Nicholson model, the particle velocity depends only on the applied electric field, $v = E\mu$, and the effective electric field for a planar geometry was defined as $E = \Delta\psi/L$.

The deposited mass will be determined by

$$m = SC_d\delta \tag{17}$$

Under these conditions, combining Eqs. (16) and (17) gives

$$m = \mu ESC_d\frac{\phi_d}{\phi_d - \phi_s}t \tag{18}$$

Comparing the Hamaker expression (Eq. (1)), where

$$C_s = \rho_p\phi_s \tag{19}$$

and the Biesheuvel and Verweij equation (Eq. (18)), where

$$C_d = \rho_p\phi_d \tag{20}$$

this theory considers the deposition dependence of the deposit growth vs. the starting solid content of the suspension, where a correction factor, X, should be incorporated to the kinetics expression for highly concentrated suspensions ($\phi_s > 0.2$ when being $\phi_d \sim 0.6$):

$$X = \frac{\phi_d}{\phi_d - \phi_s} \tag{21}$$

Subsequently, the same researchers proposed a kinetics expression based on their previous model considering the effect of concentration decrease during the deposit forming.[50] Here a stirred and diluted suspension is the studied system, so in this case they correctly considered that there is no diffusion of particles because there is not a sufficient concentration gradient. They also fix other system conditions such as considering a constant volume suspension, V, and the global electroneutrality.

Under these conditions the proposed mass balance of the particles in suspension was

$$V\frac{d\phi_s}{dt} = S(\phi_d - \phi_s)\frac{d\delta}{dt} = S(\phi_d - \phi_s)v\frac{\phi_s}{\phi_{d-}\phi_s} \tag{22}$$

Solving Eq. (22), by considering the characteristics of the described system, gives

$$\delta = \frac{V}{S}\frac{\phi_{s,0}}{\phi_d}(1 - e^{-t/\tau}) \tag{23}$$

where $\phi_{s,0}$ is the initial volumetric fraction of the suspension and τ is the characteristic time defined by Eq. (7). Considering Eqs. (4), (17), (19) and (20), Eq. (23) yields:

$$\delta = \frac{m_0}{SC_d}(1 - e^{-t/\tau}) \tag{24}$$

fitting the model proposed by Sarkar and Nicholson[22] for a similar system (Eq. (8)).

In agreement with Sarkar and Nicholson, Biesheuvel and Verweij consider that the effective electric field under potentiostatic conditions depends on the deposit electrical characteristics. In this case, the relationship between the dielectric constants of the deposit, ε_d, and suspension, ε_s, were considered and the applied electric field was defined by

$$E = \frac{\Delta\psi}{L + \delta((\varepsilon_s/\varepsilon_d) - 1)} \tag{25}$$

In addition to the Sarkar and Nicholson analyses (Eq. (15)), the authors describe how Eq. (25) predicts no deposit growth when $\varepsilon_s < \varepsilon_d$. In fact, when a low concentration is considered ($\phi_s \ll \phi_d$), the dielectric constant of the suspension can be

approximated by the dielectric constant of the liquid medium ($\varepsilon_s = \varepsilon_l$), and similarly, the dielectric constant of the deposit can be approximated by the dielectric constant of the particles ($\varepsilon_d = \varepsilon_p$). Under these limits Eq. (25) indicates that homogeneous layers can be only obtained *a priori* when the particle permittivity, ε_p, is lower than the liquid permittivity, ε_l.

To avoid the effect of the deposit resistivity increase on the effective electrical force acting on particles, Sarkar and Nicholson suggested working under galvanostatic or constant-current conditions.[22] In that way, the voltage drop across the two electrodes increases with time, but the voltage/unit distance in the suspension remains constant. Working under galvanostatic conditions Ma and Cheng in 2002[51] determined experimentally the relationship between the "kinetics parameter", k, and the applied current intensity:

$$k = k_0(e^{i/i_0} - 1) \tag{26}$$

where i (mA cm^{-2}) is the current density, and i_0 (mA cm^{-2}) and k_0 (s^{-1}) are considered the reference conditions from which the expression predicts the kinetics constant under other applied currents, facilitating more effective modelling and controlling of the process.

However, most of the experimental work in the literature describes EPD processes performed under potentiostatic or constant-voltage conditions, and hence substantial effort has been made to model the effective electric field applied for each system.[11,12,16,18,20,52–55]

Several authors have proposed different secondary phenomena occurring during the EPD process that influence the effectiveness of the applied electric field. In 1999 Van der Biest and Vanderperre,[20] introduced an expression for the potential drop over an electrophoretic cell with flat, equal surface area electrodes which consists of four terms:

$$\Delta\psi = \Delta\psi_a + \frac{I}{S\rho_d}\delta + \frac{I}{S\rho_s}L + \Delta\psi_c \tag{27}$$

where I (A) is the current and $\Delta\psi_a$ and $\Delta\psi_c$ (V) are the potential drop at the anode and cathode respectively.

So, to consider the electric field strength in a suspension as: $E = \Delta\psi/L$, the resistivity of the deposit has to be of the same order as the resistivity of the suspension, and changes in the electrode polarization and in the suspension resistivity must be negligible. However, even when the electrode is selected in order to eliminate its boundary reactions, it is still necessary to consider changes in suspension resistivity during the process.

Several authors[56,57] have considered the effect of suspension resistivity in electrophoretic feasibility. They have measured the suspension conductivity σ (S cm^{-1}) especially in suspensions stabilized by the addition of salts of different metals.[58–60] In 1996, Ferrari and Moreno studied the effect on EPD of different parameters of an aqueous suspension stabilized electrosterically.[17,61,62] These studies claimed a special role for the suspension conductivity in the effectiveness of the electrophoretic process in aqueous media. Other authors have also considered the influence of conductivity on the deposition in aqueous and non-aqueous systems.[30,58,63–76] Some of them have demonstrated that a high ionic concentration in the suspension could be deleterious for particle stability, inhibiting the movement of ceramic particles, and thereby decreasing the deposit growth and sometimes its quality. In fact, these studies indicate that electrostatic and electrosteric stabilization in non-aqueous and aqueous media have to be adjusted in order to assure a low ionic concentration in stable suspensions. Then, the effectiveness of the electrophoretic process increases because the particles are the main current carriers.

Both surface-charged particles and ions, contribute to the transport of the electric charge when an external electric field is applied to the system.[76,77] The net current is

$$I = I^+ + I^- + I_p \tag{28}$$

where I^+, I^- and I_p are the electric current (A) transported by the cations, anions and particles of the suspension respectively.

Assuming that free-ions and particles (with their ionic clouds) are homogeneously distributed in the bulk suspension, the total resistivity is

$$\rho_s = \left[\frac{1}{\rho_+} + \frac{1}{\rho_-} + \frac{1}{\rho_p}\right]^{-1} \tag{29}$$

where ρ_+, ρ_- and ρ_p represent the contribution of the cations, anions and particles respectively to the suspension resistivity.

The resistivity of the optimized suspensions mainly depends on the particle concentration. There are numerical models and theoretical expressions describing the relationship between conductivity (or resistivity) and solid content of concentrated suspensions with spherical rigid[78,79] or soft particles,[80,81] whose application is restricted to suspensions with uncharged particles. In practice, most experimental systems are formed by charged particles, where the conductivity (or resistivity) is affected by the thickness and properties of the electric double-layer or the characteristics of the polyelectrolyte adsorbed at the particle surface. The effective conductivity of dilute suspensions of charged particles was first addressed by Saville in 1983.[82] In this paper, the effect of counterions and non-specific adsorption are taken into account, and the expression proposed for the conductivity is

$$\sigma_s = \sigma_{s,\infty}(1 + \alpha\phi_s) \tag{30}$$

where the suspension conductivity, σ_s (S cm^{-1}), depends on the conductivity of the suspension liquid medium, $\sigma_{s,\infty}$ (S cm^{-1}), the volume fraction of particles in suspension, ϕ_s, and the zeta potential or double-layer thickness, α.

The proportional dependence of the suspension conductivity on solid content has been determined experimentally by different authors working on the EPD process for different powders when the suspension vehicle and the amount of dispersant were fixed.[57,61,73,77]

Recently, Anné et al.[83] have proposed a mathematical description of the kinetics based on the Hamaker model and the Biesheuvel correction for suspensions with high solid loading considering that the suspension conductivity and the current density vary during EPD under constant-voltage conditions. The expression of the electric field considering the conductivity of

the suspension is

$$E = \frac{I}{S\sigma_s} \tag{31}$$

Considering Eqs. (2) and (21):

$$\frac{dm}{dt} = f\mu \frac{I}{\sigma_s} C_s \frac{\phi_d}{\phi_d - \phi_s} \tag{32}$$

This model fits EPD results obtained from an alumina suspension prepared with ethanol considering different additives as dispersants. The proposed expression (Eq. (32)) was verified using experimental data collected during the deposition.

In 2005, Ferrari et al.[84] proposed a resistivity model for the deposition kinetics considering the relationship between colloidal parameters such as suspension concentration and resistivity (Eq. (30)) during the EPD process. This model describes experimental results, obtained for longer deposition times and for suspensions in which resistivities change significantly during the deposition process, more accurately.

Anné et al. assumed in Eq. (32) that the conduction surface was equal to the electrode deposition area and the cross-section of the EPD cell. Consequently, Eq. (32) as a function of the suspension resistivity is

$$\frac{dm}{dt} = f\mu I \rho_s C_s \tag{33}$$

On the other hand, a linear relation may be used to describe the dependence of resistivity on solid content, as follows:

$$\rho_s = \rho_{s,\infty} - (\rho_{s,\infty} - \rho_{s,0}) \frac{C_s}{C_{s,0}} \tag{34}$$

where $\rho_{s,0}$ is the initial resistivity of the suspension and $\rho_{s,\infty}$ is the resistivity at infinite time, when $C_s = 0$. Substituting Eqs. (5) and (34) into Eq. (33), a differential equation is obtained, of the form:

$$\frac{d}{dt}\left(\frac{m}{m_0}\right) = \frac{1}{\tau_0}\left(1 - \frac{m}{m_0}\right)\left(1 + \left(\frac{\rho_{s,\infty}}{\rho_{s,0}} - 1\right)\frac{m}{m_0}\right) \tag{35}$$

where the characteristic deposition time, τ_0, is similar to that in Eq. (6), and is defined by

$$\tau_0 = \frac{V}{f\mu I \rho_{s,0}} \tag{36}$$

The solution of this new equation with the same initial condition as in Eq. (6), $m(0) = 0$, is

$$m(t) = m_0\left(1 - \frac{1}{1 + (\rho_{s,0}/\rho_{s,\infty})(e^{t/\tau_\infty} - 1)}\right) \tag{37}$$

where the characteristic deposition time, τ_∞, is defined as in Eq. (36), with $\rho_{s,0} = \rho_{s,\infty}$.

According to the solution given in Eq. (37), it is evident that for long deposition times, $t \to \infty$, the deposited mass $m(t) \to m_0$, but the qualitative behaviour of the curve $m(t)$ deserves some discussion. Eq. (35) shows that

$$\frac{d}{dt}\left(\frac{m}{m_0}\right) > 0 \tag{38}$$

whatever the amount of deposited mass ($0 \le m/m_0 < 1$), so the curve $m(t)$ in Eq. (37) always increases.

Differentiating Eq. (35) again, using the same equation to eliminate the derivate, leads to:

$$\frac{d^2}{dt^2}\left(\frac{m}{m_0}\right) = \frac{1}{\tau_0^2}\left(1 - \frac{m}{m_0}\right)\left(1 + \left(\frac{\rho_{s,\infty}}{\rho_{s,0}} - 1\right)\frac{m}{m_0}\right) \times \left(\frac{\rho_{s,\infty}}{\rho_{s,0}} - 2 - 2\left(\frac{\rho_{s,\infty}}{\rho_{s,0}} - 1\right)\frac{m}{m_0}\right) \tag{39}$$

The first three factors are positive because $\rho_{s,\infty} > \rho_{s,0}$. If $\rho_{s,\infty}/\rho_{s,0} \le 2$, which includes the Sarkar and Nicholson model in which $\rho_{s,\infty}/\rho_{s,0} = 1$, the last factor will be negative and hence, $m(t)$ will rise with a continuously decreasing slope, as in a typical saturation curve. By contrast, if $\rho_{s,\infty}/\rho_{s,0} \ge 2$, the second derivate (Eq. (39)) will be positive as long as:

$$0 \le \frac{m}{m_0} < \frac{\rho_{s,\infty} - 2\rho_{s,0}}{2(\rho_{s,\infty} - \rho_{s,0})} \tag{40}$$

and will become negative above this value, thus meaning that initially the curve $m(t)$ rises with an increasing slope, producing an S-shaped saturation curve.

Converting this to deposition time using Eq. (37), the rising of the curve takes place within the range $0 \le t < T$, where

$$T = \tau_\infty \ln\left(\frac{\rho_{s,\infty}}{\rho_{s,0}} - 1\right) \tag{41}$$

The growth of the slope depends exclusively on the variation of the resistivity, and it increases as ρ_∞/ρ_0 increases. The shape

Table 1
Summary of different equations, corrections and experimental expressions proposed by different authors.

Ref	Kinetics milestones	Models or experimental expressions	Eqs.
15	Basic equation	$m = C_s \mu S E t$	(1)
22	Quantification of the deposition behaviour: the sticking factor	$dm/dt = f\mu S E C_S$	(2)
	Considering the solid loading variation	$m(t) = m_0(1 - e^{-t/\tau})$	(8)
19	Considering concentrated suspensions ($\phi_s > 0.2$)	$m = C_s \mu S E t(\phi_d/(\phi_d - \phi_s))$	(18)
22	Considering solid loading and electric field variation	$R'm(t) + (R'm_0 + L)\ln((m_0 - m(t))/m_0) + k'\Delta\psi t = 0$	(15)
51	Experimental expression determining the variation of the kinetics parameter vs. the current applied	$k = k_0(e^{i/i_0} - 1)$	(26)
83	Considering the suspension resistivity variation	$m = f\mu(I/\sigma_S)C_s(\phi_d/(\phi_d - \phi_s))$	(32)
84	Considering the linear relationship of the suspension resistivity and solid loading	$m(t) = m_0(1 - (1/1 + (\rho_{s,0}/\rho_{s,\infty})(e^{t/\tau_\infty} - 1)))$	(37)

of the $m(t)$ curve is not affected by any other parameter. This S-shaped behaviour has already been reported in the literature for long time scale EPD tests, especially for aqueous suspensions, although it also appears in non-aqueous media when deposition time is long enough.[84]

Finally, notice that if $\rho_{s,\infty} = \rho_{s,0}$ (and hence $\rho_s = \rho_{s,\infty}$ constant) the solution of this last kinetics model (Eq. (37)) reduces to the Sarkar and Nicholson model (Eq. (8)). Also, if $t \ll \tau_\infty$, this solution becomes that of the linear model proposed by Hamaker (Eq. (1)). So, Eq. (37) subsumes previous models of EPD kinetics. Table 1 summarises different equations, corrections and experimental expressions proposed by different authors.

5. Conclusions

Models developed to date consider the variation of parameters related to both suspension and electrical conditions, i.e. solid concentration and resistivity of the whole system. Other factors should now also be studied in depth, such as differences in deposition and conduction surfaces, and the deleterious effect of particle mobility during deposition time, etc. However, it is even more important to describe the surface networks developed during particle clustering, which is critical for predicting particle arrangement and designing micro- and nano-patterned materials. The electrically driven formation of arrays depends not only on the long range interaction forces (DLVO), but also on the non-DLVO interactions and liquid electrodynamic and electro-osmotic effects. Similarly, reversibility of the electrodes (substrates) plays a significant role in both transport and deposition steps. In this sense, the application of electrochemical techniques and AFM to the study of colloidal chemistry and particles sticking will be key elements of further EPD research.

Acknowledgements

This work has been supported by the Spanish Government under contract MAT2006-01038, and the Comunidad Autonoma de Madrid under contract CCG08-CSIC/MAT-3811.

References

1. Cusking, B. L., Lolessnichenki, V. L. and O'Connor, C. L., Recent advances in the liquid-phase syntheses of inorganic nanoparticles. *Chem. Rev.*, 2004, **104**, 3893–3946.
2. Rödel, J., Kounga, A. B. N., Weissenberger-Eibl, M., Koch, D., Bierwisch, A., Rossner, W. *et al.*, Development of a roadmap for advanced ceramics. *J. Eur. Ceram. Soc.*, 2009, **29**(9), 1549–1560.
3. Staiger, M., Flatt, R. J., Bowen, P. and Hofman, H., *Colloidal processing of nanosized ceramic dispersions: particle size distributions and their effect on colloid stability. Calculation and rheological behaviour*. The American Ceramic Society, Westerville, OH, 2001, pp. 173–178.
4. Corni, I., Ryan, M. P. and Boccaccini, A. R., Electrophoretic deposition: from traditional ceramics to nanotechnology. *J. Eur. Ceram. Soc.*, 2008, **28**, 1353–1367.
5. Cao, G. and Liu, D., Templated-based síntesis of nanorod, nanowire, and nanotube arrays. *Adv. Colloid Interface Sci.*, 2008, **136**, 45–64.
6. Bersa, L. and Liu, M., A review on fundamentals and applications of electrophoretic deposition (EPD). *Prog. Mater. Sci.*, 2007, **52**, 1–61.
7. Boccaccini, A., Roether, J. A., Thomas, B. J. C., Shapper, M. S. P., Chavez, E., Stoll, E. *et al.*, The electrophoretic deposition of inorganic nanoscaled materials. *J. Ceram. Soc. Jpn.*, 2006, **114**, 1–14.
8. Kershner, R. J., Bullard, J. W. and Cima, M. J., The role of electrochemical reactions during electrophoretic particle deposition. *J. Colloid Interface Sci.*, 2004, **278**, 146–154.
9. Luckham, P. F., Manipulating forces between surfaces: applications in colloid science and biophysics. *Adv. Colloid Interface Sci.*, 2004, **111**, 29–47.
10. Liang, Y., Hilal, N., Langston, P. and Starov, V., Interaction forces between colloidal particles in liquid: theory and experiment. *Adv. Colloid Interface Sci.*, 2007, **134–135**, 151–166.
11. Stappers, L., Zhang, L., Van der Biest, O. and Fransaer, J., The effect of electrolyte conductivity on electrophoretic deposition. *J. Colloid Interface Sci.*, doi:10.1016/j.jcis.2008.09.022.
12. Pignolet, C., Filiarte, C. and Foissy, A., Influence of surfactant counterions during electrophoretic particle deposition. *Langmuir*, 2008, **24**, 10181–10186.
13. Hodgson, S. N. B., Shen, X. and Sale, F. R., Electrophoretic deposition of alkaline earth coatings from EDTA complexes. *J. Mater. Sci.*, 2002, **37**, 4019–4028.
14. Negishi, H., Yamaji, K., Imura, T., Kitamoto, D., Ikegami, T. and Yanagishita, H., Electrophoretic deposition mechanism of YSZ/n-propanol suspensión. *J. Electrochem. Soc.*, 2005, **152**(2), J16–J22.
15. Hamaker, H. C., Formation of a deposit by electrophoresis. *Trans. Faraday Soc.*, 1940, **35**, 279–287.
16. Ji, C., Lan, W. and Xiao, P., Fabrication of yttria-stabilized zirconia coatings using electrophoretic deposition: packing mechanism during deposition. *J. Am. Ceram. Soc.*, 2008, **91**(4), 1102–1109.
17. Ferrari, B. and Moreno, R., Electrophoretic deposition of aqueous alumina slips. *J. Eur. Ceram. Soc.*, 1997, **17**, 549–556.
18. Anné, G., Vanmeensel, K., Vleugels, J. and Van der Biest, O., Influence of the suspension composition on the electric field and deposition rate during electrophoretic deposition. *Colloid Surf. A: Phys. Eng. Aspects*, 2004, **245**, 35–39.
19. Biesheuvel, P. M. and Verweij, H., Theory of cast formation in electrophoretic deposition. *J. Am. Ceram. Soc.*, 1999, **82**(6), 1451–1455.
20. Van der Biest, O. and Vandeperre, L. J., Electrophoretic deposition of materials. *Annu. Rev. Mater. Sci.*, 1999, **29**, 327–352.
21. Moreno, R. and Ferrari, B., Advanced ceramics via EPD of aqueous slurries. *Am. Ceram. Soc. Bull.*, 2000, **79**, 44–48.
22. Sarkar, P. and Nicholson, P. S., Electrophoretic deposition (EPD): mechanisms, kinetics, and application to ceramics. *J. Am. Ceram. Soc.*, 1996, **79**(8), 1897–2002.
23. Moreno, R., The role of slip additives in tape casting technology. Part I. Solvents and dispersants. *Am. Ceram. Soc. Bull.*, 1992, **71**, 1521–1530.
24. Van Tassel, J. J. and Randall, C. A., Ionic gradients at an electrode above the equilibrium limit current. Stabilization of ion depleted conduction by a nanoporous alumina Layer during electrophoretic deposition. *J. Phys. Chem. C*, 2007, **111**, 3358–3365.
25. Koura, N., Tsukamoto, T., Shoji, H. and Hotta, T., Preparation of various oxides films by an electrophoretic method: a study of the mechanism. *Jpn. J. Appl. Phys.*, 1995, **34**, 1643–1647.
26. Shacham, R., Mandler, D. and Avnir, D., Electrochemically induced sol–gel deposition of zirconia thin films. *Chem. Eur. J.*, 2004, **10**, 1936–1943.
27. Ma, J. and Cheng, W., Deposition and packing study of sub-micron PZT ceramics using electrophoretic deposition. *Mater. Lett.*, 2002, **56**, 721–727.
28. De, D. and Nicholson, P. S., Role of ionic depletion in deposition during electrophoretic deposition. *J. Am. Ceram. Soc.*, 1999, **82**(11), 3031–3036.
29. Pang, X., Casagrande, T. and Zhitomirsky, I., Electrophoretic deposition of hydroxyapatite–$CaSiO_3$–chitosan composite coatings. *J. Colloid Interface Sci.*, 2009, **330**(2), 323–329.
30. Popa, A. M., Vleugels, J., Vermant, J. and Van der Biest, O., Influence of surfactant addition sequence on the suspension properties and electrophoretic deposition behaviour of alumina and zirconia. *J. Eur. Ceram. Soc.*, 2006, **26**, 933–939.

31. Ferrari, B., Francisco, I. M. and Moreno, R., Ni-YSZ self-supported films by gel electrophoresis. *Ceram. Inter.*, 2005, **31**, 863–868.
32. Moreno, R. and Ferrari, B., Aqueous electrophoretic deposition of ceramics: the controlling parameters. In *Proceeding of the International Conference on Electrophoretic Deposition: Fundamentals and Applications*, ed. A. R. Boccaccini, O. Van der Biest and J. B. Talbot. The Electrochemical Society, 2002, pp. 94–1001.
33. Ristenpart, W. D., Aksay, I. A. and Saville, D. A., Assembly of colloidal aggregates by electrohydrodynamic flow: kinetic experiments and scaling análisis. *Phys. Rev.*, 2004, **E 69**, 021405.
34. Solomentsev, Y., Böhmer, M. and Anderson, J. L., Particle clustering and pattern formation during electrophoretic deposition: a hydrodynamic model. *Langmuir*, 1997, **13**, 6058–6068.
35. Solomentsev, Y., Guelcher, S. A., Bevan, M. and Anderson, J. L., Aggregation dynamics for two particles during electrophoretic deposition under steady fields. *Langmuir*, 2000, **16**, 9208–9216.
36. Kim, J., Anderson, J. L., Garoff, S. and Sides, P. J., Effects of zeta potential and electrolyte on particle interactions on an electrode under ac polarization. *Langmuir*, 2002, **18**, 5387–5391.
37. Besra, L., Uchikoshi, T., Suzuki, T. S. and Sakka, Y., Bubble-free aqueous electrophoretic deposition (EPD) by pulse-potential application. *J. Am. Ceram. Soc.*, 2008, **91**(10), 3154–3159.
38. Neirinck, B., Fransaer, J., Van der Biest, O. and Vleugels, J., Aqueous electrophoretic deposition in asymmetric AC electric fields (AC–EPD). *Electrochem. Commun.*, 2008, **11**, 57–60.
39. Gardeshzadeh, A. R., Raissi, B. and Marzbanrad, E., Preparation of Si powder thick films by low frequency alternating electrophoretic deposition. *J. Mater. Sci.*, 2008, **43**, 2507–2508.
40. Gardeshzadeh, A. R., Raissi, B. and Marzbanrad, E., Electrophoretic deposition of SnO_2 nanoparticles using low frequency AC electric fields. *Mater. Lett.*, 2008, **62**, 1697–1699.
41. Hirata, Y., Nishimoto, A. and Ishisara, Y., Forming of alumina powder by electrophoretic deposition. *J. Ceram. Soc. Jpn., Int. Ed.*, 1991, **99**, 105–109.
42. Zhang, Z., Huang, Y. and Jiang, Z., Electrophoretic deposition forming of SiC–TZP composites in a nonaqueous sol media. *J. Am. Ceram. Soc.*, 1994, **77**(7), 1946–1949.
43. Patel, M. N., Williams, R. D., May, R. A., Uchida, H., Stevenson, K. J. and Johnston, K. P., Electrophoretic deposition of Au nanocrystals inside perpendicular mesochannels of TiO_2. *Chem. Mater.*, 2008, **20**(19), 6029–6040.
44. Bao, Y. and Nicholson, P. S., Constant current electrophoretic infiltration deposition of fiber-reinforced ceramic composites. *J. Am. Ceram. Soc.*, 2007, **90**(4), 1063–1070.
45. Wang, Y. C., Leu, I. C. and Hon, M. H., Size control of ZnO nanofibril within template by electrophoretic deposition. *Electrochem. Solid-State Lett.*, 2004, **7**, D15–D18.
46. Haber, S. and Gal-Or, L., Deep electrophoretic penetration and deposition of ceramic particles inside porous substrates. I. Analytical model. *J. Electrochem. Soc.*, 1992, **139**, 1071–1077.
47. Haber, S., Liubovich, S. and Gal-Or, L., Deep electrophoretic penetration and deposition of ceramic particles inside porous substrates. II. Experimental model. *J. Electrochem. Soc.*, 1992, **139**, 1078–1081.
48. Will, J., Hruschka, M. K. M., Gubler, L. and Gauckler, L. J., Electrophoretic deposition of zirconia on porous anodic substrates. *J. Am. Ceram. Soc.*, 2001, **84**(2), 328–332.
49. Chen, C. Y., Chen, S. Y. and Liu, D. M., Electrophoretic deposition forming of porous alumina membranes. *Acta Mater.*, 1999, **47**(9), 2717–2726.
50. Gonzalez-Cuenca, M., Biesheuvel, P. M. and Verweij, H., Modeling constant voltage electrophoretic deposition from stirred suspension. *AICHE J.*, 2000, **46**(3), 626–631.
51. Ma, J. and Cheng, W., Electrophoretic deposition of lead zirconate titanate ceramics. *J. Am. Ceram. Soc.*, 2002, **85**(7), 1735–1737.
52. Ciou, S. J., Funga, K. Z. and Chiang, K. W., Behaviors and mechanism of electrolyte electrophoresis during electrophoretic deposition. *J. Power Sources*, 2008, **175**, 33–39.
53. Ciou, S. J., Funga, K. Z. and Chiang, K. W., A comparison of the artificial neural network model and the theoretical model used for expressing the kinetics of electrophoretic deposition of YSZ on LSM. *J. Power Sources*, 2008, **175**, 338–344.
54. Anné, G., Neirinck, B., Vanmeensel, K., Van der Biest, O. and Vleugels, J., Origin of the potential drop over the deposit during electrophoretic deposition. *J. Am. Ceram. Soc.*, 2006, **89**(3), 823–828.
55. Wang, Y. C., Leu, I. C. and Hon, M. H., Kinetics of electrophoretic deposition for nanocrystalline zinc oxide coatings. *J. Am. Ceram. Soc.*, 2004, **87**(1), 84–88.
56. Vander Poorten, H., Caracterisation de l'élèctrodeposition et des élèctrodêpots de pâtes ceramiques. *Silicates Ind.*, 1981, **41**(9), 159–172.
57. Choudhary, J. Y., Ray, H. S. and Rai, K. N., Electrophoretic deposition of alumina from aqueous suspensions. *Trans. J. Br. Ceram. Soc.*, 1982, **81**, 193–196.
58. Shane, M. J., Talbot, J. B., Schreiber, R. D., Ross, C. L., Sluzky, E. and Hesse, K. R., Electrophoretic deposition of Phosphors. I. Conductivity and zeta potential measurements. *J. Colloid Interface Sci.*, 1994, **165**, 325–333.
59. DeBeer, E., Duval, J. and Meulenkamp, E. A., Electrophoretic deposition: a quantitative model for particle deposition and binder formation from alcohol-based suspensions. *J. Colloid Interface Sci.*, 2000, **222**, 117–124.
60. Bouyer, F. and Foissy, A., Electrophoretic deposition of silicon carbide. *J. Am. Ceram. Soc.*, 1999, **82**(8), 2001–2010.
61. Moreno, R. and Ferrari, B., Effects of the slurry properties on the homogeneity of alumina deposits obtained by aqueous electrophoretic deposition. *Mater. Res. Bull.*, 2000, **35**(6), 887–897.
62. Ferrari, B. and Moreno, R., The conductivity of aqueous Al_2O_3 slips for electrophoretic deposition. *Mater. Lett.*, 1996, **28**, 353–355.
63. Uchikoshi, T. and Sakka, Y., Phosphate esters as dispersants for the cathodic electrophoretic deposition of alumina suspensions. *J. Am. Ceram. Soc.*, 2008, **91**(6), 1923–1926.
64. Javidi, M., Javadpour, S., Bahrololoom, M. E. and Ma, J., Electrophoretic deposition of natural hydroxyapatite on medical grade 316L stainless steel. *Mater. Sci. Eng. C*, 2008, **28**, 1509–1515.
65. Sun, H., Quan, X., Chen, S., Zhao, H. and Zhao, Y., Preparation of well-adhered g-Al_2O_3 washcoat on metallic wire mesh monoliths by electrophoretic deposition. *Appl. Surface Sci.*, 2007, **253**, 3303–3310.
66. Plešingerová, B., Súèik, G., Maryška, M. and Horkavcová, D., Hydroxyapatite coatings deposited from alcohol suspensions by electrophoretic deposition on titanium substrate. *Ceramics-Silikáty*, 2007, **51**(1), 15–23.
67. Tang, F., Uchikoshi, T., Ozawa, K. and Sakka, Y., Effect of polyethylenimine on the dispersion and electrophoretic deposition of nano-sized titania aqueous suspensions. *J. Eur. Ceram. Soc.*, 2006, **26**, 1555–1560.
68. Lebrette, S., Pagnoux, C. and Abeland, P., Fabrication of titania dense layers by electrophoretic deposition in aqueous media. *J. Eur. Ceram. Soc.*, 2006, **26**, 2727–2734.
69. Doungdaw, S., Uchikoshi, T., Noguchic, Y., Eamchotchawalit, C. and Sakka, Y., Deposition of lead zirconate titanate (PZT) powder from ethanol suspension prepared with phosphate ester. *Sci. Technol. Adv. Mater.*, 2005, **6**, 927–932.
70. Wang, C., Ma, J. and Cheng, W., Formation of polyetheretherketone polymer coating by electrophoretic deposition method. *Surf. Coat. Technol.*, 2003, **173**, 271–275.
71. Ma, J., Wang, C. and Peng, K. W., Electrophoretic deposition of porous hydroxyapatite scaffold. *Biomaterials*, 2003, **24**, 3505–3510.
72. Wang, C., Ma, J., Cheng, W. and Zhang, R., Thick hydroxyapatite coatings by electrophoretic deposition. *Mater. Lett.*, 2002, **57**, 99–105.
73. Yamada, N., Shoji, H., Kubo, Y. and Katayama, S., Preparation of inorganic–organic hybrid films containing particles using electrophoretic deposition method. *J. Mater. Sci.*, 2002, **37**, 2071–2076.
74. Ogata, N., Van Tassel, J. and Randall, C. A., Electrode formation by electrophoretic deposition of nanopowders. *Mater. Lett.*, 2000, **49**, 7–14.
75. Chen, F. and Liu, M., Preparation of YSZ films on LSM and LSM-YSZ substrates using an electrophoretic deposition process. *J. Eur. Ceram. Soc.*, 2001, **21**, 127–134.
76. Tang, F. Q., Uchikoshi, T., Ozawa, K. and Sakka, Y., Electrophoretic deposition of aqueous nano-γ-Al_2O_3 suspensions. *Mater. Res. Bull.*, 2003, **37**, 653–660.

77. Put, S., Veugels, J. and Van der Biest, O., Gradient profile prediction in functionally graded materials processed by electrophoretic deposition. *Acta Mater.*, 2003, **51**, 6303–6317.
78. Carrique, F., Arroyo, F. J. and Delgado, A. V., Electrokinetics of concentrated suspensions of spherical colloidal particles: effect of a dynamic stern layer on electrophoresis and DC conductivity. *J. Colloid Interface Sci.*, 2001, **243**, 351–361.
79. Oshima, H., Electrical conductivity of a concentrated suspension of spherical colloidal particles. *J. Colloid Interface Sci.*, 1999, **212**, 443–448.
80. Oshima, H., Electrical conductivity of a concentrated suspension of soft particles. *J. Colloid Interface Sci.*, 2000, **229**, 307–309.
81. Jonhson, T. J. and Davis, E. J., An analysis of electrophoresis of concentrated suspensions of colloidal particles. *J. Colloid Interface Sci.*, 1999, **215**, 397–408.
82. Saville, D. A., The electrical conductivity of suspensions of charged particles in ionic solutions: the role of added counterions and nonspecific adsortion. *J. Colloid Interface Sci.*, 1983, **91**(1), 34–50.
83. Anné, G., Vanmeensel, K., Vleugels, J. and Van der Biest, O., A mathematical description of the kinetics of the electrophoretic deposition process for Al_2O_3-based suspensions. *J. Am. Ceram. Soc.*, 2005, **88**(8), 2036–2039.
84. Ferrari, B., Moreno, R. and Cuesta, J. A., A resistivity model of electrophoretic deposition. *Key Eng. Mater.*, 2006, **314**, 175–180.